

Kinetic and DFT Studies on the Mechanism of C–S Bond Formation by Alkyne Addition to the $[\text{Mo}_3\text{S}_4(\text{H}_2\text{O})_9]^{4+}$ Cluster

Jose Ángel Pino-Chamorro,[†] Andrés G. Algarra,^{†,§} M. Jesús Fernández-Trujillo,[†] Rita Hernández-Molina,[‡] and Manuel G. Basallote^{*,†}

[†]Departamento de Ciencia de los Materiales e Ingeniería Metalúrgica y Química Inorgánica, Facultad de Ciencias, Universidad de Cádiz, Apartado 40, Puerto Real, 11510 Cádiz, Spain

[‡]Departamento de Química Inorgánica e Instituto Universitario de Bio-Orgánica “Antonio González”, Universidad de La Laguna, La Laguna, 38200 Tenerife, Islas Canarias, Spain

S Supporting Information

ABSTRACT: Reaction of $[\text{Mo}_3(\mu_3\text{-S})(\mu\text{-S})_3]$ clusters with alkynes usually leads to formation of two C–S bonds between the alkyne and two of the bridging sulfides. The resulting compounds contain a bridging alkenedithiolate ligand, and the metal centers appear to play a passive role despite reactions at those sites being well illustrated for this kind of cluster. A detailed study including kinetic measurements and DFT calculations has been carried out to understand the mechanism of reaction of the $[\text{Mo}_3(\mu_3\text{-S})(\mu\text{-S})_3(\text{H}_2\text{O})_9]^{4+}$ (**1**) cluster with two different alkynes, 2-butyne-1,4-diol and acetylenedicarboxylic acid. Stopped-flow experiments indicate that the reaction involves the appearance in a single kinetic step of a band at 855 or 875 nm, depending on the alkyne used, a position typical of clusters with two C–S bonds. The effects of the concentrations of the reagents, the acidity, and the reaction medium on the rate of reaction have been analyzed. DFT and TD-DFT calculations provide information on the nature of the product formed, its electronic spectrum and the energy profile for the reaction. The structure of the transition state indicates that the alkyne approaches the cluster in a lateral way and both C–S bonds are formed simultaneously.

■ INTRODUCTION

The formation of carbon–sulfur bonds is of interest both in industry and in biological systems,¹ and metal complexes have been found to promote those processes, with Mo often the metal center.² Although most examples are mono or dinuclear complexes, trinuclear $[\text{M}_3(\mu_3\text{-Q})(\mu\text{-Q})_3]^{4+}$ clusters (M = Mo, W; Q = O, S, Se) have also been shown to lead to formation of C–S bonds. These clusters are stable in acidic solutions in air,³ and this has facilitated studies on the formation of acetylene-cluster adducts, the Mo compounds being more reactive than their W analogues.⁴ Thus, $[\text{Mo}_3(\mu_3\text{-S})(\mu\text{-X})(\mu\text{-S})_2(\text{H}_2\text{O})_9]^{4+}$ (X = O, S) clusters react with acetylene in 1 M HCl yielding $[\text{Mo}_3(\mu_3\text{-S})(\mu\text{-X})(\mu\text{-SCH=CHS})(\text{H}_2\text{O})_9]^{4+}$ (X = O, S) compounds which contain alkenedithiolate ligands resulting from the formation of two C–S bonds.⁵ In contrast, the $[\text{W}_3(\mu_3\text{-S})(\mu\text{-X})(\mu\text{-S})_2(\text{H}_2\text{O})_9]^{4+}$ (X = O, S) clusters do not react with acetylene in the same medium.⁶ The nature of ligands substituting the coordinated water molecules in the starting cluster has been also found to affect the capability of activating the alkyne, $[\text{W}_3(\mu_3\text{-S})(\mu\text{-O})(\mu\text{-S})_2(\text{NCS})_9]^{5-}$ being more reactive than its aquo analogue.⁶ These results indicate that the reactivity of these clusters toward the acetylene molecule or its derivatives change considerably depending on the metal, the bridge atoms, or the ligands.⁷ On the other hand, the reaction is not limited to acetylene, and examples exist of C–S bond formation with different substituted acetylenes as dimethylacetylenedicarboxylate and acetylenedicarboxylic acid.^{7,8} Although compounds resulting from the formation of two C–S bonds appear to be the starting point in the chemistry of these compounds, inspection of the crystal structures solved for this kind of adduct reveals that there are compounds that

may be classified according to the three different structural types in Figure 1. Examples of compounds corresponding to the different types are given in Table 1.

Whereas the synthetic and structural aspects are reasonably well established, the mechanistic information on these processes is very limited. Shibahara and co-workers⁹ have proposed that compounds of type I are generated by the concerted formation of two C–S bonds, and protonation of type I adducts leads to type II, with a single C–S bond, while type III is formed by addition of a second alkyne to a type II compound. The proposal of a concerted initial attack to form type I adducts is made by analogy to the results obtained in related studies with dinuclear molybdenum compounds.¹⁰ However, detailed kinetic-mechanistic studies are still missing despite the fact that formation of all these adducts leads to large changes in the electronic spectrum, which presumably should facilitate kinetic studies. Actually, there are in the literature semiquantitative observations concerning the duration of the reaction, the required temperature and the acidity of the reaction medium.⁹ In the case of $[\text{Mo}_3(\mu_3\text{-S})(\mu\text{-X})(\mu\text{-S})_2(\text{H}_2\text{O})_9]^{4+}$ (X = O, S), the reaction occurs in hours at room temperature, whereas for $[\text{W}_3(\mu_3\text{-S})(\mu\text{-S})_3(\text{NCS})_9]^{5-}$ the reaction takes days and increasing the solution pH makes it even slower. Importantly, to our knowledge there is no report of compound resulting from alkyne addition to $\mu\text{-O}$ or $\mu_3\text{-S}$ atoms, and the role of the metal center appears to be innocent, except for one singular case reported by Hidai and co-workers.¹¹

Received: September 16, 2013

Published: November 22, 2013



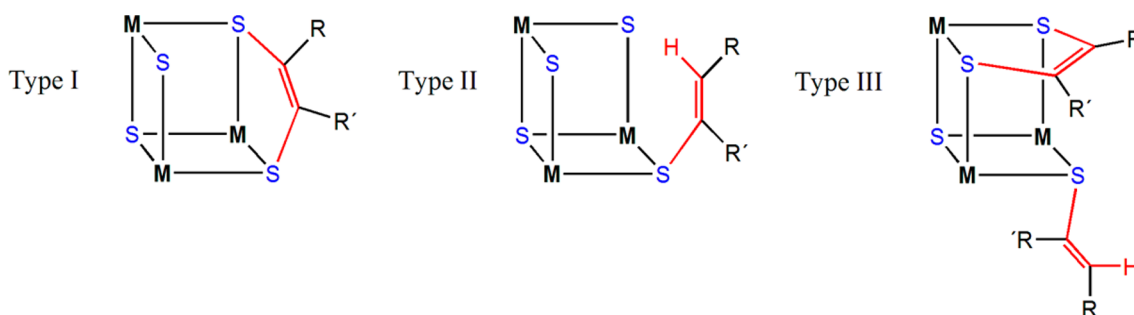


Figure 1. Structural types reported in the literature for products resulting of the addition of alkynes to M_3S_4 clusters.

Table 1. Bibliographic Information on the Cluster Reaction Products Resulting of the Addition of Alkynes to M_3Q_4 Clusters

structure type	compound	alkyne $R-C\equiv C-R'$	references
Type I	$[Mo_3(\mu_3-S)(\mu-X)(\mu-S)_2(H_2O)_9]^{4+}$ X = O, S	R = R' = H	5
	$[Mo_3(\mu_3-S)(\mu-S)_3(Hnta)]^{4+}$ Hnta = nitrilotriacetate	R = R' = H	7
Type II	$[W_3(\mu_3-S)(\mu-O)(\mu-S)_2(NCS)_9]^{4+}$	R = R' = H	6
Type III	$[W_3(\mu_3-S)(\mu-S)_3(NCS)_9]^{5-}$	R = R' = H	9
	$W_3(\mu_3-S)(\mu-S)_3(\mu-OAc)(dtp)_3(CH_3CN)$ dtp = diethyldithiophosphate	R = R' = CO ₂ Me	9
	$[Mo_3(\mu_3-S)(\mu-S)_3(Hnta)]^{4+}$ Hnta = nitrilotriacetate	R = R' = CO ₂ H	7

Continuing with our interest in mechanistic studies of this type of cluster, we decided to carry out kinetic studies on these reactions. The cluster selected was the $[Mo_3(\mu_3-S)(\mu-S)_3(H_2O)_9]^{4+}$ aqua cluster, and the reaction was studied in concentrated acidic solutions using two different entering alkynes: 2-butyne-1,4-diol (*btd*) and acetylenedicarboxylic acid (*adc*). The kinetic studies are complemented with DFT and TD-DFT calculations that allow making a mechanistic proposal for the formation of type I adducts and anticipate future studies aimed to confirm and refine the mechanistic proposal, thus facilitating rationalization of these alkyne activation processes.

EXPERIMENTAL SECTION

General Remarks. Solutions of the $[Mo_3S_4(H_2O)_9]^{4+}$ cluster in 2 M HCl or Hpts were prepared following the literature procedure.¹² The UV–vis spectra of those solutions show bands at 370 and 616 nm with molar absorptivities of 4995 and 326 $\epsilon/M^{-1} \text{ cm}^{-1}$, respectively.

Kinetic Experiments. The kinetic experiments were carried out with an Applied Photophysics SX-17MV stopped-flow spectrometer provided with a PDA1 photodiode array (PDA) detector, and a Cary 50 Bio UV–vis spectrophotometer. All experiments were carried out at 25.0 °C by mixing an aqueous solution of $[Mo_3S_4(H_2O)_9]^{4+}$ with another solution containing an excess of the alkyne (*btd* or *adc*). The range of alkyne concentrations was 0.01–0.05 M, enough to ensure pseudo-first-order conditions. The ionic strength was kept constant in all cases at 2.0 M by adding the required amounts of Hpts, HCl, LiCl, or Lipts solutions (*pts*[−] = *p*-toluenesulfonate). The complex solutions were prepared at concentrations of ca. 8×10^{-4} M in HCl or Hpts 2.0 M, and preliminary experiments at two different complex concentrations were carried out to confirm the first order dependence of the observed rate constants on the complex concentration. The cluster concentration was estimated from the UV–vis spectra, and the Hpts concentration was determined by titration with KOH (phenolphthalein indicator). In all cases the spectral changes were measured over a wide wavelength range and analyzed with program Specfit.¹³ Satisfactory fits were obtained using a kinetic model with a single kinetic step.

Computational Details. All theoretical calculations were performed using GAUSSIAN 09 (rev. A.02)¹⁴ together with the B3LYP functional,¹⁵ and in order to avoid complications associated with the formation of deprotonated species of *adc*, they were restricted to the reaction between $[Mo_3S_4(H_2O)_9]^{4+}$ and *btd*. Optimizations were carried out with the effects of the solvent (H_2O , $\epsilon = 78.39$)

included self-consistently through the PCM method,¹⁶ employing the SDD relativistic ECP and associated basis set for Mo and S atoms,¹⁷ with added polarization functions for the latter ($\zeta = 0.503$),¹⁸ and 6-31g** basis set for C, O, and H atoms.¹⁹ The nature of all described species was confirmed via analytical frequency calculations as either minima (all positive eigenvalues) or transition states (one negative eigenvalue), and IRC calculations and subsequent geometry optimizations were used to confirm the minima linked by each transition state.

All energies shown refer to Gibbs free energies in solution, and were obtained by adding zero-point and thermal effects at 298.15 K, as well as dispersion effects (D3),²⁰ to the electronic energies computed by single-point calculations on the previously optimized structures with a larger basis set system, and also including solvent effects (PCM).¹⁶ This basis set system differs only from the one used during the optimizations in the employment of 6-311+G(2d,2p) for C, O, and H atoms.

The absorption electronic spectra of the previously optimized species were obtained by means of TD-DFT methods²¹ and 40 monoexcitations were calculated for each species. The basis set system employed was the same as for the optimizations, and the solvent effects were included via the polarizable continuum model (PCM).¹⁶ GaussSum 2.2 was used to draw the absorption spectra.²² The equation employed by the program to calculate the theoretical spectrum and the extinction coefficients is based on Gaussian convolution and is reported in the open source code of the program (available at <http://gausssum.sourceforge.net/>). The full width at half-maximum value used for the simulated spectrum was 1500 cm^{-1} .

RESULTS AND DISCUSSION

Kinetic Studies. The reaction of the $[Mo_3(\mu_3-S)(\mu-S)_3(H_2O)_9]^{4+}$ cluster (1) with 2-butyne-1,4-diol (*btd*) in 2 M HCl occurs with spectral changes in the stopped-flow time scale that involve changes in the band of the starting cluster at 616 nm and the appearance of a new band at 875 nm. These changes are illustrated in Figure 2 and can be satisfactorily fitted with a model including a single kinetic step (see Figure S1). Experiments at longer reaction times using a conventional UV–vis spectrophotometer show the disappearance of the band at 875 nm, but this step occurs in a much larger time scale (thousands of minutes) and is accompanied by precipitation, which precluded a kinetic study of this latter process and hindered characterization by NMR of the product resulting

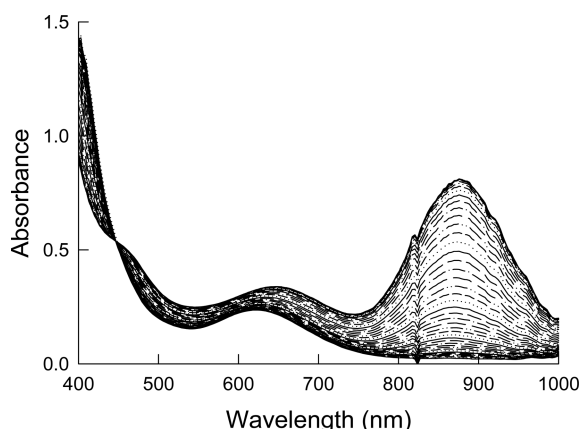


Figure 2. Typical spectral changes for the reaction of cluster **1** with *btd* in aqueous medium 2 M HCl. ($T = 25.0\text{ }^{\circ}\text{C}$, $[\mathbf{1}] = 8 \times 10^{-4}\text{ M}$, $[\textit{btd}] = 0.03\text{ M}$; time base = 100 s).

from the initial attack by the alkyne. The near-infrared band is typical of reaction products between this kind of cluster and alkynes with formation of two bonds C–S,^{5,9} so that the stopped-flow experiments provide information about the process of alkyne activation. Similar results were obtained using other concentrations of HCl with the ionic strength kept at 2.0 M by addition of LiCl. In this way, kinetic studies were performed at four different concentrations of HCl: 0.5, 1.0, 1.5, and 2.0 M. The spectral changes when the cluster reacts with an excess of acetylenedicarboxylic acid (*adc*) are also similar, although the band for the reaction product appears at 850 nm instead of 875 nm, and the reaction is remarkably faster (Figure S2). In all cases the spectral changes can be satisfactorily fitted by a single exponential, and their amplitudes are independent of the concentration of added alkyne, which indicates that the reaction occurs under conditions of irreversibility.

For both alkynes the values of the rate constant (k_{obs}) show a linear dependence with the alkyne concentration (Figure 3),

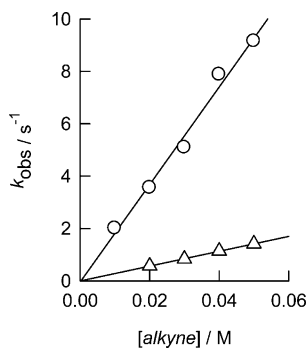


Figure 3. Plot of the dependence of $[\textit{alkyne}]$ on the rate constants for the reaction of **1** with *btd* (triangles) and *adc* (circles) in aqueous solution 2 M HCl. The solid lines correspond to the fit of data using the eq 1. The data for the reaction with *btd* have been multiplied by 10.

and fitting to eq 1 leads to the values of the second order constant (k) shown in Table 2. The table indicates that the kinetics does not change significantly when changing the proton concentration, the average value for the four series of experiments in HCl/LiCl media being $k = 2.9 \pm 0.1\text{ M}^{-1}\text{ s}^{-1}$ and $k = 169 \pm 7\text{ M}^{-1}\text{ s}^{-1}$ for *btd* and *adc*, respectively. The independence of the rate constants with respect to the acid

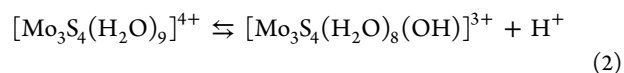
Table 2. Summary of the Second-Order Rate Constants (k , in $\text{M}^{-1}\text{ s}^{-1}$) Obtained for the Reaction of the Cluster with an Excess of Alkynes *btd* and *adc* to $25.0\text{ }^{\circ}\text{C}$ in the Presence of Different Concentrations of Acid (HCl or *Hpts*)^a

medium	<i>btd</i> ($X = \text{Cl}^-$)	<i>btd</i> ($X = \textit{pts}^-$)	<i>adc</i> ($X = \text{Cl}^-$)	<i>adc</i> ($X = \textit{pts}^-$)
2.0 M HX	2.83 ± 0.01^b	1.94 ± 0.03	164 ± 3	46.8 ± 1.0
1.5 M HX	2.88 ± 0.04	1.93 ± 0.03	166 ± 5	42.7 ± 1.5
1.0 M HX	3.05 ± 0.08	1.89 ± 0.03	179 ± 8	43.3 ± 1.3
0.5 M HX	3.05 ± 0.04	1.92 ± 0.02	166 ± 5	45.7 ± 1.0

^aThe ionic strength was kept constant in all cases at 2.0 M by adding of the necessary amounts of LiCl or *Lipts*. ^bIn experiments carried out using an excess of cluster, the value obtained is $k_1 = 3.3 \pm 0.4\text{ M}^{-1}\text{ s}^{-1}$.

concentration is surprising because both the cluster and the alkyne may have acid–base equilibria. Thus, the cluster has been shown to form a hydroxocomplex (eq 2) with a $\text{p}K_a$ value of 0.66,²³ which indicates that the solutions used for kinetic studies contain up to 10–30% of hydroxocomplex. With regard to the alkyne, although *btd* ($\text{p}K_a$ of 12.7)²⁴ does not show any equilibrium at the acid concentrations used in the kinetic studies, the $\text{p}K_a$ for the two carboxylic groups of *adc* are very low: $\text{p}K_{a1} = 0.66\text{--}1.74$ and $\text{p}K_{a2} = 2.34\text{--}4.38$.²⁵ According to these values, the major species in the kinetic experiments is the diprotonated form, but significant amounts of the other species will be formed when the concentration of protons decreases. As these concentration changes are not paralleled by changes in the rate constant, it must be concluded that the three species ($\text{H}_2\textit{adc}$, Hadc^- , and adc^{2-}) react at the same rate. With regard to the cluster, the kinetic results would also indicate that the hydroxocomplex reacts at a rate similar to that of the acuocomplex. However, as the experiments were carried out in the presence of an excess of chloride ions, formation of chlorocomplexes is expected to occur²⁶ and this can lead to changes of the $\text{p}K_a$ to values that could make negligible the amount of hydroxocomplex formed.

$$k_{\text{obs}} = k[\textit{alkyne}] \quad (1)$$



To ascertain the possible effect of chloride, experiments were also carried out using *Hpts* instead of HCl. The reaction also occurs in the time scale of the stopped-flow, with kinetics quite similar to that observed in HCl medium, although the bands are shifted to 600 nm for the starting compound, and to 840 and 820 nm for the reaction products with *btd* and *adc*, respectively. Those changes are consistent with changes in the nature of the starting cluster from $[\text{Mo}_3\text{S}_4\text{Cl}_x(\text{H}_2\text{O})_{9-x}]^{(4-x)+}$ in HCl to $[\text{Mo}_3\text{S}_4(\text{H}_2\text{O})_9]^{4+}$ in *Hpts* medium. The values of k in 2.0 M *Hpts*/*Lipts* media are also included in Table 2. They are independent of the acid concentration and the mean values are $1.92 \pm 0.02\text{ M}^{-1}\text{ s}^{-1}$ for *btd* and $45 \pm 2\text{ M}^{-1}\text{ s}^{-1}$ for *adc*. Both values are smaller than those found in HCl/LiCl media and so it must be concluded that the chlorocomplexes react faster than the acu and hydroxo complexes. However, the differences are not very large, i.e., the changes in the coordination sphere of the metal centers do not lead to large effects on the kinetics of reaction with alkynes, which suggests that the metal centers do not participate directly in the interaction with the alkyne during the course of the reaction.

An interesting kinetic feature of reactions with these clusters is the frequent observation of statistical kinetics. Its occurrence in reactions of substitution of coordinated water in aqua clusters was reported many years ago by Sykes and co-workers,^{23,27} and confirmed more recently using diode-array detection and global analysis of kinetic data at multiple wavelengths.²⁸ Examples of statistical kinetics, and of small deviations from it, have been also reported for reactions of proton transfer to coordinated hydride in clusters containing diphosphines.²⁹ The numerical aspects of statistical kinetics in reactions of these clusters have been described in detail in a recent publication,²⁸ so that only a brief comment is given here. Thus, from a formal point of view, it consists of a simplification of the kinetics when the three equivalent metal centers behave as independent chromophores and react sequentially with rate constants which follow the statistical factors 3:2:1. In that case, the expected three consecutive exponentials are simplified to a single one with an apparent rate constant that corresponds to reaction at the third metal center. Although the reaction of alkynes leads to products in which there is no reaction with the metal centers, the transient participation of Mo atoms cannot be ruled out completely. Furthermore, as the cluster also contains equivalent sulfur atoms, it would be possible to observe statistical kinetics for the reaction on these atoms. Since a way to detect the appearance of statistical kinetics consists in comparing rate constants obtained using an excess of cluster with those obtained in the presence of an excess of the other reagent, experiments with *btd* in 2 M HCl were also performed with a deficit of alkyne. To keep the cluster in excess with the stock solution available, the alkyne concentration had to be reduced to 2.5×10^{-5} M. Under those conditions the reaction rate decreases and the plot of k_{obs} vs the cluster concentration (Figure 5) shows that the rate constant deviates from a linear fit

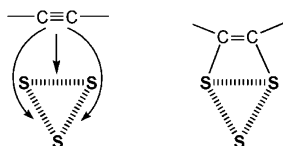


Figure 4. Illustrating the possibilities of alkyne attack at the triangle defined by the three μ_2 -S atoms in cluster **1**. Although there are three equivalent sites for the initial approach of one alkyne, once the first two C–S bonds are formed there is no possibility of equivalent attacks at the remaining sites because there is a single S not involved in C–S bonds.

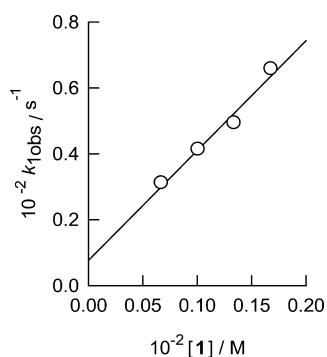


Figure 5. Plot of the dependence of the rate constants for the reaction of cluster **1** with a deficit of *btd* in 2 M HCl. The solid line corresponds to the fit of data using eq 3.

through the origin, indicating that the process now occurs under conditions of reversibility, surely because the cluster excess is not enough to cause complete conversion to the product. The fit of the data to eq 3 leads to $k_{-1} = (8 \pm 4) \times 10^{-4} \text{ s}^{-1}$ and $k_1 = 3.3 \pm 0.4 \text{ M}^{-1} \text{ s}^{-1}$, the second order rate constant being in agreement with that obtained for the same concentration of HCl using an excess of alkyne ($k_1 = 2.83 \text{ M}^{-1} \text{ s}^{-1}$). This finding indicates that there is no statistical kinetics and that the measured rate constants correspond to a reaction with 1:1 stoichiometry between the two reactants, which suggests again that there is no transient coordination of the alkynes to the metal centers during the reaction, i.e., C–S bond formation occurs without participation of the metal atoms. In addition, operation of statistical kinetics for alkyne attack to a single bridging S can be also ruled out. In contrast, this finding supports a simultaneous attack at two μ_2 -S because, although there are three equivalent sites of attack, the attack of one alkyne molecule hinders an equivalent attack at the remaining sites (see Figure 4) and reaction occurs with 1:1 stoichiometry.

$$k_{1,\text{obs}} = k_1[1] + k_{-1} \quad (3)$$

DFT Studies. The experimental results show that **1** reacts with alkynes to form products with an intense band between 800 and 900 nm in their electronic spectra, typical of products resulting from the addition of alkynes to two sulfur atoms of this type of cluster.^{5,9} However, as these compounds can undergo further transformations in solution, DFT calculations were carried out to model the three structural types described in the literature for these products (Figure 1) and then their electronic spectra were estimated by means of TD-DFT calculations. The alkyne used in the calculations was *btd* to avoid the need of considering forms with different protonation states. The geometries and spectra obtained are included in Figures 6 and 7, respectively.

Comparison of DFT-optimized and X-ray structures of **1** shows very good agreement, with their calculated and experimental spectra being also similar. On the other hand, inspection of the spectra calculated for the three possible reaction products indicates that only the spectrum of the type I adduct agrees well with the experimental spectrum. Indeed, calculations predict the appearance of a band slightly below 900 nm, with intensity significantly higher than that shown by the starting compound. Thus, calculations support the fact that the reaction product is the result of the formation of two C–S bonds between the alkyne and the cluster, as indicated in Figure 8. With regard to the nature of the transition responsible for the appearance of the intense band between 800 and 900 nm in product type I, the calculations indicate that it is mainly associated with the HOMO \rightarrow LUMO + 1 transition, which involves charge transfer from the alkyne to the cluster core (see Figure 9), although both molecular orbitals are delocalized between several atoms of the cluster (see Supporting Information).

The stabilization achieved with formation of the reaction product is of $12.6 \text{ kcal mol}^{-1}$. It must be noted that the reaction occurs at two μ_2 -S, and attempts to obtain similar products involving interaction with one μ_2 -S and μ_3 -S lead to geometries in which there is no interaction between the alkyne and μ_3 -S, in agreement with the absence of that interaction in the crystal structures reported for this kind of compounds. A comparison between the calculated geometries for the reactant and the product reveals an elongation of the Mo–S bonds when the S atoms interact with the alkyne (see Figure 6). There is also an

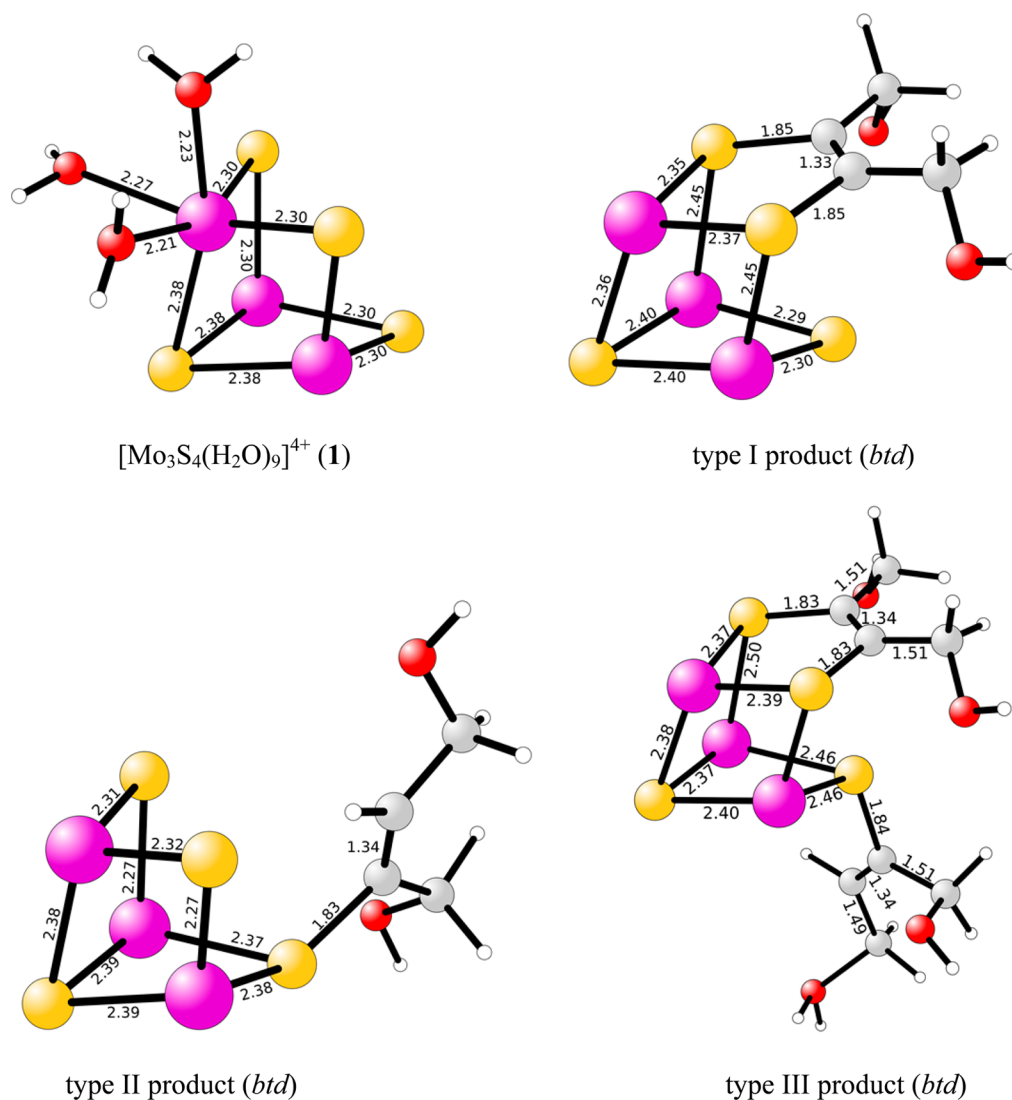


Figure 6. Computed structures and key distances (Å) of $[\text{Mo}_3\text{S}_4(\text{H}_2\text{O})_9]^{4+}$ cluster (top left) and the corresponding reaction products with *btd* showing the three types of geometry described in the literature for its reaction with alkynes (type I – top right, type II – bottom left, and type III – bottom right). H_2O molecules have been omitted for clarity (full coordinates are given in the Supporting Information), except for those coordinated to one of the Mo centers in $[\text{Mo}_3\text{S}_4(\text{H}_2\text{O})_9]^{4+}$, included for comparison with the X-ray structure, which shows average distances: Mo-O = 2.18 Å; Mo- $\mu_3\text{S}$ = 2.33 Å; Mo- $\mu_2\text{S}$ = 2.28 Å.³⁰ Color code: purple = Mo; yellow = S; gray = C; red = O; white = H.

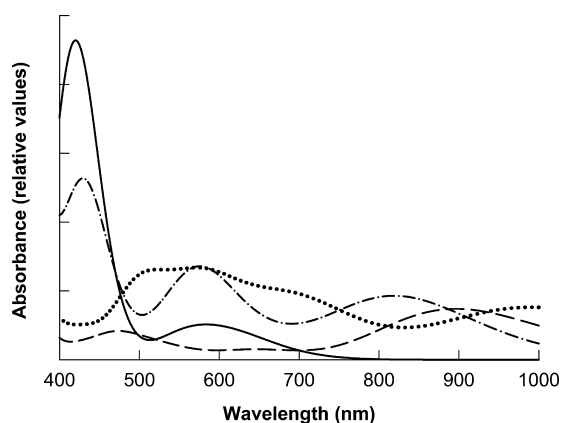


Figure 7. Calculated spectra for the starting cluster 1 (solid line) and its reaction products with *btd* showing the three types of geometries described in the literature (type I – dashed line, type II – dotted-dashed line, and type III – dotted line).

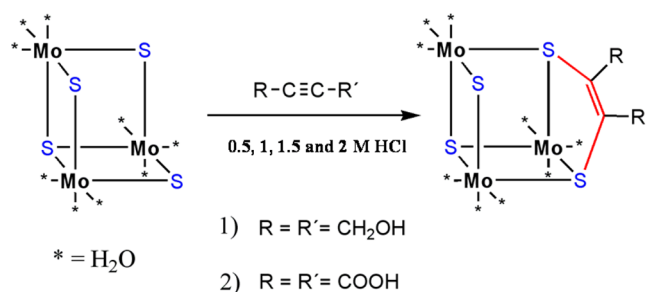


Figure 8. Representation of the reaction of cluster 1 with the alkynes *btd* and *adc*. The water molecules have been replaced by asterisks to simplify the figure.

elongation of the carbon-carbon bond of the alkyne and a significant decrease in the S-Mo-S angles, especially for the two sulfurs interacting with the alkyne (98.3° in the product *cf.* 84.7° in 1). All these structural changes are related to the need of accommodating the structure to the cluster-alkyne

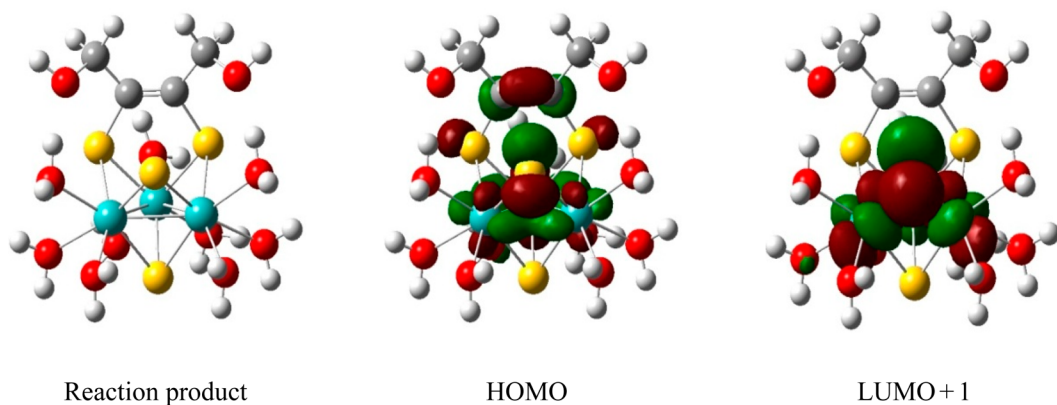


Figure 9. Computed structure of the reaction product between **1** and *btd*, and its HOMO and LUMO + 1 orbitals (isovalue = 0.04). Color code: cyan = Mo; yellow = S; gray = C; red = O; white = H.

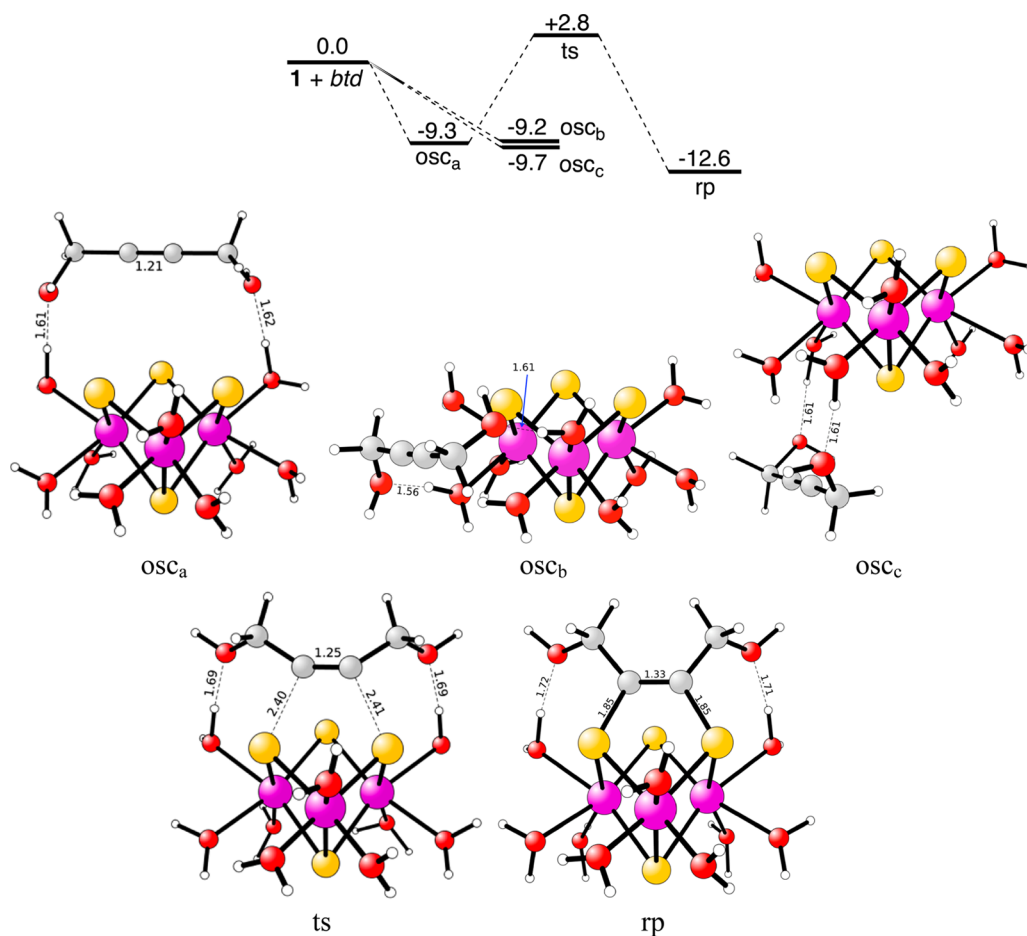


Figure 10. Computed free energy profile (kcal/mol) for the reaction between *btd* and **1**, with the structures (Å) of outer-sphere complexes (osc), transition state (ts), and reaction product (rp). Color code: green = Cl; purple = Mo; yellow = S; gray = C; red = O; white = H.

interaction, and similar reorganizations have been previously observed for other reactions of this kind of cluster.³¹ The possibility of a substitution reaction in which the alkyne substitutes one of the coordinated water molecules was also explored, but it was found that formation of the substitution product only leads to an stabilization of 5.0 kcal mol⁻¹, so that this process is unfavored against that leading to formation of the C–S bonds.

The energy profile for the formation of the type I product was also calculated. For this purpose, the geometry of a series of

outer-sphere complexes (osc) that result from the approach of the alkyne to different areas of cluster **1** was first computed (see Figure 10). Importantly, all these species are stabilized by H-bonding interactions between the hydroxyl groups of *btd* and water molecules of **1**, leading to very similar formation free energies. Among them, osc_a shows the appropriate relative alkyne-cluster orientation for the formation of the reaction product with two C–S bonds, and from this species the transition state for such conversion was subsequently located. The structure of this transition state shows that the alkyne

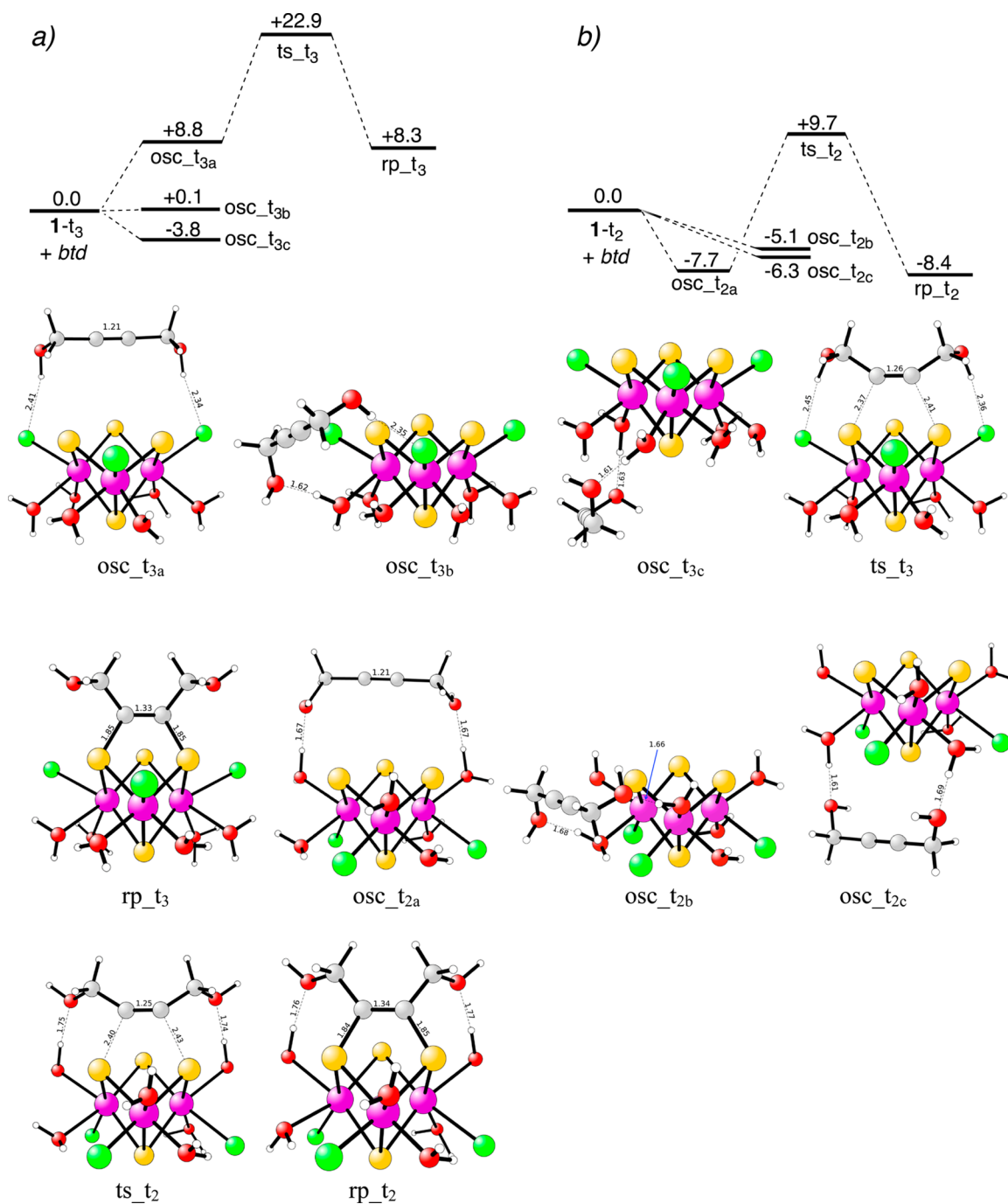


Figure 11. Computed free energy profile (kcal/mol) for the reaction between *btd* and $[\text{Mo}_3\text{S}_4\text{Cl}_3(\text{H}_2\text{O})_6]^+$, with Cl ligands *trans* to $\mu_3\text{-S}$ (1- t_3 , a), and *trans* to $\mu_2\text{-S}$ (1- t_2 , b), with the structures (Å) of outer-sphere complexes (osc), transition states (ts), and products (rp). Note that in the case of 1- t_3 , higher-energy osc featuring OH...Cl interactions are not shown for simplicity (included in the Supporting Information). Color code: green = Cl; purple = Mo; yellow = S; gray = C; red = O; white = H.

approaches laterally to the cluster to allow for simultaneous interaction with the two sulfurs, adopting a symmetrical arrangement with C–S distances of 2.40 and 2.41 Å. The computed activation barrier is 12.5 kcal/mol relative to osc_o, so calculations agree with experimental observations in the sense that the reaction occurs in the stopped-flow time scale, in a single kinetic step, and without direct participation of the metal centers.

Lastly, theoretical calculations were also carried out to gain insight into the possible effects caused by chloride coordination. The formation of chlorocomplexes upon reaction of cluster 1

with an excess of Cl^- is well established in the literature. However, there are some discrepancies with regard to the site of substitution. Whereas the early kinetic and NMR studies³² indicated the preferential substitution of water coordinated *trans* to $\mu_2\text{-S}$, the crystal structures available correspond to substitutions *trans* to $\mu_3\text{-S}$.²⁶ In a recent kinetic and DFT study²⁸ we found that substitution of water *trans* to $\mu_2\text{-S}$ is favored from both the thermodynamic and kinetic points of view. However, the calculated energies are not very different for substitution at both sites and the difference can be compensated by the hydrogen bonds formed with cucurbituril

in the adducts characterized by X-ray. The spatial arrangement of cucurbituril favors the formation of a network of hydrogen bonds with coordinated water molecules *trans* to μ_2 -S, so that Cl^- coordination would be forced to occur *trans* to μ_3 -S. We think that the whole set of information available can be interpreted considering that substitution occurs *trans* to μ_2 -S, but in the presence of cucurbituril it can be followed by slower isomerization to give the crystallographically characterized adducts containing coordinated chlorides *trans* to μ_3 -S. In the absence of cucurbituril, the reaction products will show preferential substitution at sites *trans* to μ_2 -S. In any case, to explore the possible effects of coordinated chlorides on the alkyne activation process, calculations similar to those summarized in Figure 10 were carried out using $\text{Mo}_3\text{S}_4\text{Cl}_3(\text{H}_2\text{O})_6^+$, both with the three chlorides *trans* to μ_3 -S and μ_2 -S (labeled as I-t₃ and I-t₂ respectively). The derived free energy profiles and computed structures are shown in Figure 11. Interestingly, the alkyne (*btd*) can now form H-bonding interactions with water molecules of the clusters (similar to those with 1), or with chloride ligands, although these are found to be less favored thermodynamically. As can be seen in Figure 11a, OH...Cl interactions strongly affect the reaction with I-t₃ because the formation of the reaction product (rp_t₃) requires a relative alkyne-cluster orientation in which those interactions are present throughout. Overall, the process becomes endergonic and the energy barrier is found to be significantly higher than in the absence of chloride. In contrast, when the Cl^- ligands are *trans* to μ_2 -S (I-t₂, Figure 11b) the reaction can still go through a series of species that only feature alkyne-water H-bonding interactions, and the structures of outer-sphere complex (osc_t_{2a}), transition state (ts_t₂), and reaction product (rp_t₂) compare very well with those in Figure 10. The process is also thermodynamically favored and an energy barrier of 17.4 kcal/mol is computed. Although this indicates that chlorocomplexes should react with alkynes more slowly than the aquacluster, the experimental results show that they actually react slightly faster, a discrepancy that presently we are not able to explain.

CONCLUSION

The mechanistic studies carried out in the present work on the addition of alkynes to an M_3S_4 cluster have revealed that the addition of a molecule of alkyne occurs in the stopped-flow time scale with a single kinetic step. Theoretical calculations suggest that the reaction occurs with the lateral approach of the alkyne to the cluster to allow for the simultaneous interaction with two μ_2 -S. In the transition state, the carbon-carbon triple bond weakens at the same time that the two C-S bonds begin to form. These conclusions basically coincide with those previously proposed by Shibahara et al.^{5,7} on the basis of qualitative observations, and provide a starting point for the analysis and rationalization of the different factors that can affect to the formation of the C-S bonds: the nature of the cluster, the alkyne, and the solvent, as well as the possibility of further transformations leading to compounds labeled type II and III in Figure 1.

ASSOCIATED CONTENT

Supporting Information

Plots showing the electronic spectra calculated for the reaction of 1 with *btd* and spectral changes for the reaction of 1 with *adc*. Cartesian coordinates and absolute energies for all optimized structures. For the three products of the reaction between

cluster 1 and *btd* in Figure 6, plots of their frontier molecular orbitals as well as tables with their TD-DFT calculated transition energies, oscillator strength, and major orbital contributions. This material is available free of charge via the Internet at <http://pubs.acs.org>.

AUTHOR INFORMATION

Corresponding Author

*Tel: +34 956-012739; E-mail: manuel.basallote@uca.es.

Present Address

[§]Department of Organic Chemistry, Arrhenius Laboratory, Stockholm University, SE-10691 Stockholm, Sweden.

Notes

The authors declare no competing financial interest.

ACKNOWLEDGMENTS

Financial support by Junta de Andalucía (Grupo FQM-137, Grant P07-FQM-02734) and the Spanish MICINN and EU FEDER program (projects CTQ2009-14443-C01 and C02, and CTQ2012-37821-C01 and C02) is gratefully acknowledged. Helpful comments by the reviewers are also acknowledged.

REFERENCES

- (1) Rakowski Dubois, M. *Chem. Rev.* **1989**, *89*, 1.
- (2) (a) Coucouvanis, D.; Hadjikyriacou, A.; Toupadakis, A.; Koo, S. M.; Ileperuma, O.; Draganjac, M.; Salifoglou, A. *Inorg. Chem.* **1991**, *30*, 754. (b) Coucouvanis, D.; Hadjikyriacou, A.; Draganjac, M.; Kanatzidis, M. G.; Ileperuma, O. *Polyhedron* **1986**, *5*, 349. (c) Draganjac, M.; Coucouvanis, D. *J. Am. Chem. Soc.* **1983**, *105*, 139. (d) Pilato, R. S.; Eriksen, K. A.; Greaney, M. A.; Stiefel, E. I.; Goswami, S.; Kilpatrick, L.; Spiro, T. G.; Taylor, E. C.; Rheingold, A. L. *J. Am. Chem. Soc.* **1991**, *113*, 9372. (e) Halbert, T. R.; Pan, W. H.; Stiefel, E. I. *J. Am. Chem. Soc.* **1983**, *105*, 5476. (f) Schollhammer, P.; Cabon, N.; Capon, J.-F.; Pétilion, F. Y.; Talarmin, J.; Muir, K. W. *Organometallics* **2001**, *20*, 1230.
- (3) (a) Shibahara, T. *Adv. Inorg. Chem.* **1991**, *37*, 143. (b) Saito, T. In *Early Transition Metal Clusters with π -Donor Ligands*, Chisholm, M. H., Ed.; VCH: New York, 1995.
- (4) (a) Llusar, R.; Uriel, S. *Eur. J. Inorg. Chem.* **2003**, 1271. (b) Shibahara, T. *Coord. Chem. Rev.* **1993**, *123*, 73.
- (5) Shibahara, T.; Sakane, G.; Mochida, S. *J. Am. Chem. Soc.* **1993**, *115*, 10408.
- (6) Maeyama, M.; Sakane, G.; Pierattelli, R.; Bertini, I.; Shibahara, T. *Inorg. Chem.* **2001**, *40*, 2111.
- (7) Takagi, H.; Ide, Y.; Shibahara, T. *C. R. Chimie* **2005**, *8*, 985.
- (8) Ide, Y.; Shibahara, T. *Inorg. Chem.* **2007**, *46*, 357.
- (9) Ide, Y.; Sasaki, M.; Maeyama, M.; Shibahara, T. *Inorg. Chem.* **2004**, *43*, 602.
- (10) McKenna, M.; Wright, L. L.; Miller, D. J.; Tanner, L.; Haltiwanger, R. C.; Rakowski DuBois, M. *J. Am. Chem. Soc.* **1983**, *105*, 5329.
- (11) Ikada, T.; Mizobe, Y.; Hidai, M. *Organometallics* **2001**, *20*, 4441.
- (12) Sokolov, M. N.; Coichev, N.; Moya, H. D.; Hernandez-Molina, R.; D., B. C.; Sykes, A. G. *J. Chem. Soc., Dalton Trans.* **1997**, *11*, 1863.
- (13) Binstead, R. A.; Jung, B.; Zuberbühler, A. D. *SPECFIT-32*; Spectrum Software Associates, Chappel Hill, 2000.
- (14) Frisch, M. J.; Trucks, G. W.; Schlegel, H. B.; Scuseria, G. E.; Robb, M. A.; Cheeseman, J. R.; Scalmani, G.; Barone, V.; Mennucci, B.; Petersson, G. A.; Nakatsuji, H.; Caricato, M.; Li, X.; Hratchian, H. P.; Izmaylov, A. F.; Bloino, J.; Zheng, G.; Sonnenberg, J. L.; Hada, M.; Ehara, M.; Toyota, K.; Fukuda, R.; Hasegawa, J.; Ishida, M.; Nakajima, T.; Honda, Y.; Kitao, O.; Nakai, H.; Vreven, T.; Montgomery, J. A. J.; Peralta, J. E.; Ogliaro, F.; Bearpark, M.; Heyd, J. J.; Brothers, E.; Kudin, K. N.; Staroverov, V. N.; Kobayashi, R.; Normand, J.; Raghavachari, K.; Rendell, A.; Burant, J. C.; Iyengar, S. S.; Tomasi, J.; Cossi, M.; Rega, N.; Millam, J. N.; Klene, M.; Knox, J. E.; Cross, J. B.; Bakken, V.;

Adamo, C.; Jaramillo, J.; Gomperts, R.; Stratmann, R. E.; Yazyev, O.; Austin, A. J.; Cammi, R.; Pomelli, C.; Ochterski, J. W.; Martin, R. L.; Morokuma, K.; Zakrzewski, V. G.; Voth, G. A.; Salvador, P.; Dannenberg, J. J.; Dapprich, S.; Daniels, A. D.; Farkas, O.; Foresman, J. B.; Ortiz, J. V.; Cioslowski, J.; Fox, D. I. *Gaussian09*; Gaussian, Inc., Wallingford, CT, 2009.

(15) (a) Becke, A. D. *J. Chem. Phys.* **1993**, *98*, 5648. (b) Lee, C. T.; Yang, W. T.; Parr, R. G. *Phys. Rev. B* **1988**, *37*, 785.

(16) (a) Tomasi, J.; Mennucci, B.; Cammi, R. *Chem. Rev.* **2005**, *105*, 2999. (b) Cossi, M.; Scalmani, G.; Rega, N.; Barone, V. *J. Chem. Phys.* **2002**, *117*, 43.

(17) Andrae, D.; Haussermann, U.; Dolg, M.; Stoll, H.; Preuss, H. *Theor. Chim. Acta* **1990**, *77*, 123.

(18) Hollwarth, A.; Bohme, M.; Dapprich, S.; Ehlers, A. W.; Gobbi, A.; Jonas, V.; Kohler, K. F.; Stegmann, R.; Veldkamp, A.; Frenking, G. *Chem. Phys. Lett.* **1993**, *208*, 237.

(19) (a) Harihanan, P. C.; Pople, J. A. *Theor. Chim. Acta* **1973**, *28*, 213. (b) Hehre, W. J.; Ditchfield, K.; Pople, J. A. *J. Chem. Phys.* **1972**, *56*, 2257.

(20) Grimme, S. *J. Comput. Chem.* **2006**, *27*, 1787.

(21) (a) Dreuw, A.; Head-Gordon, M. *Chem. Rev.* **2005**, *105*, 4009. (b) Burke, K.; Werschnik, K. J.; Gross, E. K. U. *J. Chem. Phys.* **2005**, *123*, 062206.

(22) O'Boyle, N. M.; Tenderholt, A. L.; Langner, K. M. *J. Comput. Chem.* **2008**, *29*, 839.

(23) Routledge, C. A.; Sykes, A. G. *J. Chem. Soc., Dalton Trans.* **1992**, 325.

(24) Fernández Díaz, L. M. Ph. D. Thesis, University of Hamburg, 2008.

(25) (a) Schwartz, L. M.; Gelb, R. I.; Laufer, D. A. *J. Chem. Eng. Data* **1980**, *25*, 95. (b) Ashton, H. W.; Partington, J. R. *Trans. Faraday Soc.* **1934**, *30*, 598. (c) Charton, M. *J. Org. Chem.* **1961**, *26*, 735.

(26) (a) Chubarova, E. V.; Samsonenko, D. G.; Platas, J. H.; Sokolov, M. N.; Fedin, V. P. *J. Struct. Chem.* **2004**, *45*, 906. (b) Chubarova, E. V.; Sokolov, M. N.; Samsonenko, D. G.; Vicent, C.; Fedin, V. P. *J. Struct. Chem.* **2006**, *47*, 939.

(27) Nasreldin, M.; Olatunji, A.; Dimmock, P. W.; Sykes, A. G. *J. Chem. Soc., Dalton Trans.* **1990**, 1765.

(28) Algarra, A. G.; Fernández-Trujillo, M. J.; Basallote, M. G. *Chem.—Eur. J.* **2012**, *18*, 5036.

(29) (a) Basallote, M. G.; Feliz, M.; Fernández-Trujillo, M. J.; Llusar, R.; Safont, V. S.; Uriel, S. *Chem.—Eur. J.* **2004**, *10*, 1463. (b) Algarra, A. G.; Basallote, M. G.; Feliz, M.; Fernández-Trujillo, M. J.; Llusar, R.; Safont, V. S. *Chem.—Eur. J.* **2006**, *12*, 1413. (c) Algarra, A. G.; Basallote, M. G.; Feliz, M.; Fernández-Trujillo, M. J.; Guillamón, E.; Llusar, R.; Vicent, C. *Inorg. Chem.* **2006**, *45*, 5576. (d) Algarra, A. G.; Basallote, M. G.; Fernández-Trujillo, M. J.; Feliz, M.; Guillamón, E.; Llusar, R.; Sorribes, I.; Vicent, C. *Inorg. Chem.* **2010**, *49*, 5935.

(30) Akashi, H.; Shibahara, T.; Kuroya, H. *Polyhedron* **1990**, *9*, 1671.

(31) Algarra, A. G.; Feliz, M.; Fernández-Trujillo, M. J.; Llusar, R.; Safont, V. S.; Vicent, C.; Basallote, M. G. *Chem.—Eur. J.* **2009**, *15*, 4582.

(32) (a) Sellsell, D. M.; Borman, C. D.; D., K. C.; Sykes, A. G. *Inorg. Chem.* **1996**, *35*, 173. (b) Richens, D. T.; Pittet, P.-A.; Merbach, A. E.; Humanes, M.; Lamprecht, G. J.; Ooi, B.-L.; Sykes, A. G. *J. Chem. Soc., Dalton Trans.* **1993**, 2305. (c) Ooi, B.-L.; Sykes, A. G. *Inorg. Chem.* **1989**, *28*, 3799. (d) Kathirgamanathan, P.; Soares, A. B.; Richens, D. T.; Sykes, A. G. *Inorg. Chem.* **1985**, *24*, 2950. (e) Ooi, B. L.; Sykes, A. G. *Inorg. Chem.* **1988**, *27*, 310. (f) Richens, D. T.; Helm, L.; Pittet, P. A.; Merbach, A. E.; Nicolo, F.; Chapuis, G. *Inorg. Chem.* **1989**, *28*, 1394.